Vol.41 No.3 June 2024 ISSN 0289-0003

ZOOLOGICAL SCIENCE

ZOOLOGICAL SCIENCE **41**: 281–289 (2024)

Volume X-ray Micro-Computed Tomography Analysis of the Early Cephalized Central Nervous System in a Marine Flatworm, *Stylochoplana pusilla*

Takanori Ikenaga[1], Aoshi Kobayashi[2], Akihisa Takeuchi[3], Kentaro Uesugi[3], Takanobu Maezawa[4], Norito Shibata[4], Tatsuya Sakamoto[2], and Hirotaka Sakamoto[2,5]*

[1]*Graduate School of Science and Engineering, Kagoshima University, Kagoshima 890-0065, Japan*
[2]*Ushimado Marine Institute (UMI), Faculty of Environmental, Life, Natural Science and Technology, Okayama University, Ushimado, Setouchi, Okayama 701-4303, Japan*
[3]*Japan Synchrotron Radiation Research Institute/SPring-8, Hyogo 679-5198, Japan*
[4]*Department of Integrated Science and Technology, National Institute of Technology, Tsuyama College, Tsuyama, Okayama 708-8509, Japan*
[5]*Department of Biology, Faculty of Environmental, Life, Natural Science and Technology, Okayama University, Kita-ku, Tsushimanaka, Okayama 700-8530, Japan*

Platyhelminthes are a phylum of simple bilaterian invertebrates with prototypic body systems. Compared with non-bilaterians such as cnidarians, the bilaterians are likely to exhibit integrated free-moving behaviors, which require a concentrated nervous system "brain" rather than the distributed nervous system of radiatans. Marine flatworms have an early cephalized 'central' nervous system compared not only with non-bilaterians but also with parasitic flatworms or freshwater planarians. In this study, we used the marine flatworm *Stylochoplana pusilla* as an excellent model organism in Platyhelminthes because of the early cephalized central nervous system. Here, we investigated the three-dimensional structures of the flatworm central nervous system by the use of X-ray micro-computed tomography (micro-CT) in a synchrotron radiation facility. We found that the obtained tomographic images were sufficient to discriminate some characteristic structures of the nervous system, including nerve cords around the cephalic ganglion, mushroom body-like structures, and putative optic nerves forming an optic commissure-like structure. Through the micro-CT imaging, we could obtain undistorted serial section images, permitting us to visualize precise spatial relationships of neuronal subpopulations and nerve tracts. 3-D micro-CT is very effective in the volume analysis of the nervous system at the cellular level; the methodology is straightforward and could be applied to many other non-model organisms.

Key words: bilaterians, micro-CT scan, central nervous system, Platyhelminthes, marine flatworms

INTRODUCTION

Bilaterians have a head- and a tail-end as well as a dorsal and ventral surface; therefore, they also have a left and a right side. Thus, compared with non-bilaterians such as cnidarians, the bilaterians are likely to exhibit integrated free-moving behaviors, which require a concentrated nervous system rather than the distributed nervous system of radiatans (Strausfeld et al., 2016; Heger et al., 2021; Martin-Duran and Hejnol, 2021). Platyhelminthes, including marine flatworms (Polycladida), are one group of simple bilaterian invertebrates; they have a simple body system: no vascular-circulatory system, no body cavity, and a mouth and anus that are morphologically identical (Noreña et al., 2015). In contrast, they do have an organized "brain" as a central nervous system (Keenan et al., 1981; Reuter et al., 1998; Quiroga et al., 2015). In Platyhelminthes, parasitic flatworms (schistosomes, tapeworms, etc.) and freshwater planarians are useful as medical/regeneration models. On the other hand, marine flatworms without a complete regenerative ability do have a well-established "brain" compared to these model planarians (Le et al., 2021; Schadt et al., 2021).

All animal organs, including the brain, have a complex three-dimensional (3-D) structure, and a comprehensive understanding of this is critical in various fields of biology. Confocal microscopy and two-photon microscopy with fluorescence labeling are often used to investigate their 3-D structure. However, autofluorescence from the mucus and

* Corresponding author. E-mail: hsakamo@okayama-u.ac.jp
doi:10.2108/zs230082

pigments of marine flatworms have made it particularly difficult to investigate their 3-D structure by use of whole-mount preparations (Pladillon et al., 2007; Bickmeyer et al., 2020). In this study, therefore, we aimed to establish a foundation for understanding brain evolution by conducting a 3-D analysis of the brains of marine flatworms, which are in the early stages of centralization but are relatively well-established "brains" within the phylum Platyhelminthes. Furthermore, 3-D analysis by micro-computed tomography (micro-CT) can be performed in various cross-sections and repeated at various angles in the desired cross-sectional plane from the same dataset. Comparison with the results of sections with various tissue stains is therefore easy and fits well with these established methods, including immunohistochemistry and DAPI staining, etc.

Preparation of serial sections followed by light microscopy observation is the traditional method for investigating the cellular organization of animal tissues and organs. This, with image-manipulating programs, has enabled us to reconstruct their 3-D structure. However, it is challenging to prepare undistorted whole serial sections in order to obtain rigorous 3-D tomographic images (Hayworth et al., 2014; Henny et al., 2014). In addition, because the plane of the serial sections is not constant, the acquired images must be aligned on the computer, which is significantly time-consuming (Hayworth et al., 2014; Henny et al., 2014). X-ray micro-CT has been used to produce 3-D images of organs in order to observe their 3-D structure without any destruction. Several studies to analyze the central nervous system with micro-CT have been performed in both vertebrates (Babaei et al., 2016; Udagawa et al., 2019; Camilieri-Asch et al., 2020) and invertebrates (Steinhoff et al., 2017; Sakurai and Ikeda, 2019; Rivera-Quiroz and Miller, 2022). Still, no study has yet provided images with cellular resolution. Recently, X-ray micro-CT in a synchrotron radiation facility has enabled us to obtain higher-resolution 3-D images of whole brains (Mizutani and Suzuki, 2012). Although tomographic images of the *Drosophila* brain stained by the reduced-silver impregnation method have allowed for the visualization of individual cells and nerve tracts (Mizutani et al., 2007, 2013), until now, there have been no reports of this methodology being applied to other invertebrate organisms, including marine flatworms, by using a synchrotron radiation facility.

Here, we report the 3-D structures of the entire central nervous system in a marine flatworm (*Stylochoplana pusilla*) by use of X-ray micro-CT in a synchrotron radiation facility (SPring-8, Hyogo, Japan). This 3-D micro-CT study has proved effective in the stereoanatomy analysis of the central nervous system at the cellular level.

MATERIALS AND METHODS

Animals

Marine flatworms, *Stylochoplana pusilla*, from the Ushimado seashore (Okayama, Japan) of the Seto Inland Sea, were used in this study. Adult *S. pusilla* (3–5 mm in body length) living symbiotically in conchs (*Monodonta confusa*) were captured from the wild. Flatworms were maintained at a temperature of 23–25°C in filtered seawater and were fed brine shrimps (nauplii of *Artemia* spp.) once every 3 days before use. *Stylochoplana pusilla* were handled, maintained, and used in accordance with the Guidelines for Animal Experimentation established by Okayama University; in accordance with international standards on animal welfare; and in compliance with national regulations. All experiments in this study were carried out on at least three different animals with similar results.

Histological procedure

Adult *S. pusilla* were immersion-fixed in 4% paraformaldehyde in 0.1 M phosphate buffer overnight at 4°C, then dehydrated through graded ethanol concentrations, cleared in lemosol, and embedded in paraffin wax. Serial sections of each specimen were cut horizontally on an HM 325 microtome (Leica, Wetzlar, Germany) at 7 μm in thickness. The paraffin sections were stained with hematoxylin-eosin (H-E) according to the established method.

Immunofluorescence

For immunofluorescence, sections were soaked in xylene three times for 5 min each to remove paraffin wax, then in a decreasing series of ethanol concentrations, and washed with phosphate-buffered saline (PBS: pH 7.4). After blocking nonspecific binding components with 1% normal goat serum and 1% bovine serum albumin in PBS containing 0.3% Triton X-100 for 30 minutes at room temperature, the sections were incubated with a primary mouse monoclonal antibody raised against *Drosophila* synapsin (3C11, Hybridoma Bank, University of Iowa, IA) (RRID: AB_528479) (1:100) or a rabbit polyclonal antiserum against acetylated-α-tubulin (Santa Cruz Biotechnology, Dallas, TX) (RRID: AB_628409) (1:250) for 1 hour at room temperature and overnight at 4°C. The synapsin antibody has previously been shown to be specific in freshwater planarians (Bischof et al., 2020). The tubulin antiserum has previously been shown to be specific in marine flatworms (Kobayashi et al., 2022). Alexa Fluor 488-linked anti-mouse IgG or Alexa Fluor 488-linked anti-rabbit IgG (Molecular Probes, Eugene, OR) was used at a dilution of 1:1000 for 1 hour at room temperature. Immunostained sections were mounted on slides with Fluoromount G, including DAPI (SouthernBiotech, Birmingham, AL), and observed by confocal laser scanning microscopy (Fluoview FV1000, Olympus, Tokyo, Japan).

X-ray micro-CT

Adult *S. pusilla* were fixed as described above and then immersed in 0.3% phosphotungstic acid (PTA) in 70% ethanol for 6–7 hours at room temperature. The specimens were washed in 70% ethanol, dehydrated, and embedded in paraffin wax as described above. X-ray micro-CT scanning was performed at the undulator beamline BL20XU at SPring-8 (proposal no. 2013A1161, 2013A1547), a synchrotron radiation facility in Hyogo, Japan, as described previously (Ikenaga et al., 2022). The energy of the X-ray beam was 10 keV. Paraffin-embedded flatworm samples were attached to the tip of wooden toothpicks and mounted on the rotation stage. Transmission X-ray images were acquired by use of a visible-light conversion unit for X-rays (AA50, Hamamatsu Photonics, Shizuoka, Japan) and a complementary metal-oxide-semiconductor (CMOS) camera (ORCA-Flash4.0, Hamamatsu Photonics). The viewing field was 2048 × 2048 pixels, and the effective pixel size was 0.5 × 0.5 μm. In total, 900 projection images were recorded with 0.2° rotation steps and a 200 ms exposure time. After X-ray micro-CT imaging, a convolution back-projection method was used to reconstruct transverse plane images. The spatial resolution of these images was estimated at 1.0–1.2 μm under similar experimental conditions (Mizutani et al., 2015). Reconstructed serial tomographic images were then processed by using the Amira image processing program (Thermo Fisher Scientific, Waltman, MA).

Ethics statement

All experimental procedures were approved in accordance with the Guide for the Care and Use of Laboratory Animals prepared by

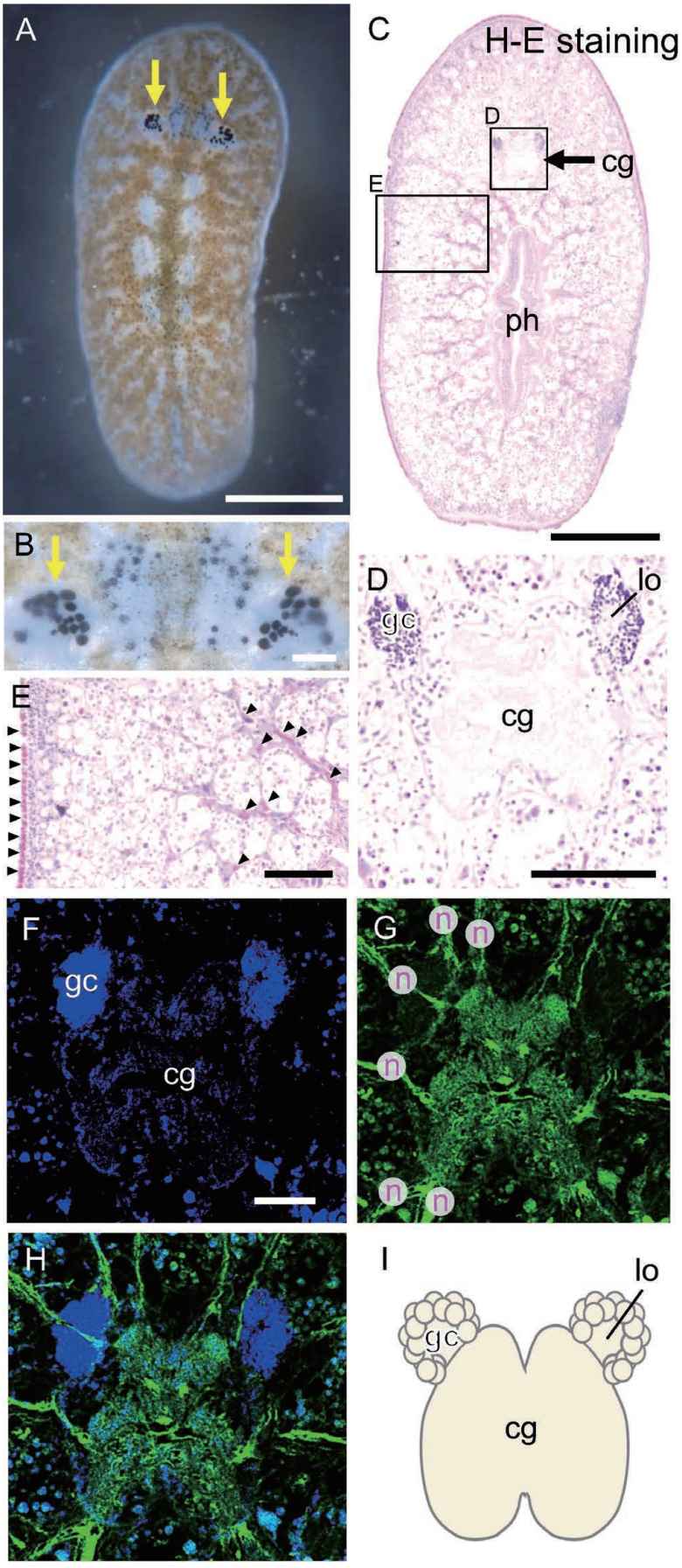

Okayama University (Okayama, Japan. http://www.cc.okayama-u.ac.jp/~animal/committee.html), although an individual ID of approval was not provided because we used only marine flatworms for the experiments in this study. All efforts were made to minimize animal suffering and reduce the number of animals used in this study. The study design, including experimental animals, experimental procedures, and statistical methods, is described in compliance with the ARRIVE guidelines.

RESULTS

Gross morphology of *S. pusilla*

Figure 1A shows a dorsal view of the marine polyclad flatworm, *Stylochoplana pusilla*. These animals have many eye points bilaterally near the midline of the anterior region of the body (Fig. 1A, B). In H-E stained horizontal sections, the cephalized central nervous tissue (cephalic ganglion) was evident in the anterior area (possibly a head) of the body (Fig. 1C, D), as reported previously for other polyclad flatworms (Quiroga et al., 2015), but not for freshwater planarians (Tricladida). Unlike insects, no such ganglion is observed in other parts of the body in the marine flatworm. The pharynx was located in the center of the body (Fig. 1C). Numerous cells densely stained with eosin were distributed radially around the pharynx and associated with the epithelium (Fig. 1E). Immunohistochemistry for acetylated-α-tubulin mainly visualized the nerve-fiber bundle-like projections, including probable six nerve cords on the left hemisphere (Fig. 1F–H).

X-ray micro-CT analysis of marine flatworms

To visualize the *S. pusilla* nervous system, we treated formaldehyde-fixed tissues of *S.*

Fig. 1. Gross morphology of the marine flatworm *Stylochoplana pusilla*. **(A, B)** Dorsal view of *S. pusilla*. Yellow arrows in **(A, B)** indicate eye-points. Upper is anterior. **(B)** Higher magnification image of the cephalic ganglion between the eye-points. **(C)** Horizontal histological sections of *S. pusilla* stained with hematoxylin-eosin (H-E) staining. The arrow in **(C)** indicates the cephalic ganglion (cg). ph: pharynx. **(D)** and **(E)** are higher magnification images of boxed areas in **(C)**. **(D)** The mushroom body-like structure, including globuli cell (gc) masses and the associated nerve bundles (lobe: lo) are located antero-lateral to the cephalic ganglion. **(E)** Numerous cells densely stained with eosin are distributed radially around the pharynx and associated with the epithelium (arrowheads). **(F–H)** Fluorescence images of horizontal sections from *Stylochoplana pusilla* cephalic ganglion region: globuli cells (gc) are stained by DAPI (blue); the axonal projections (n) are visualized by anti-acetylated-α-tubulin antibody (green). **(I)** Schematic drawing of the cephalic ganglion with the mushroom body-like structures. Scale bars = 1 mm in **(A)**, 500 μm in **(C)**, 100 μm in **(B, D, E)**, and 50 μm in **(F)**.

pusilla with a solution containing PTA before the micro-CT scanning procedure. In our study, the PTA impregnation produced excellent contrast with low background in the reconstructed tomographic images throughout the tissues of *S. pusilla* (Fig. 2). The contrast between the different tissues and cells was enhanced, and each could be distinguished, perhaps due to differences in X-ray absorbance and immersion affinity for PTA. In tomographic horizontal plane images of the anterior part of *S. pusilla*, the cephalic ganglion was located anterior to the pharynx (Fig. 2A). Six putative nerve cords on the left hemisphere that emerged from the more ventral region of the cephalic ganglion could also be recognized in horizontal plane images (Fig. 2B, and see Supplementary Movie S1). From the micro-CT analysis data, images of planes of different orientations can be derived from the same dataset. Figure 2C shows a representative transverse plane image obtained from the same dataset as Figs. 2A and B. In this plane, the cephalic ganglion also appeared as an encapsulated structure.

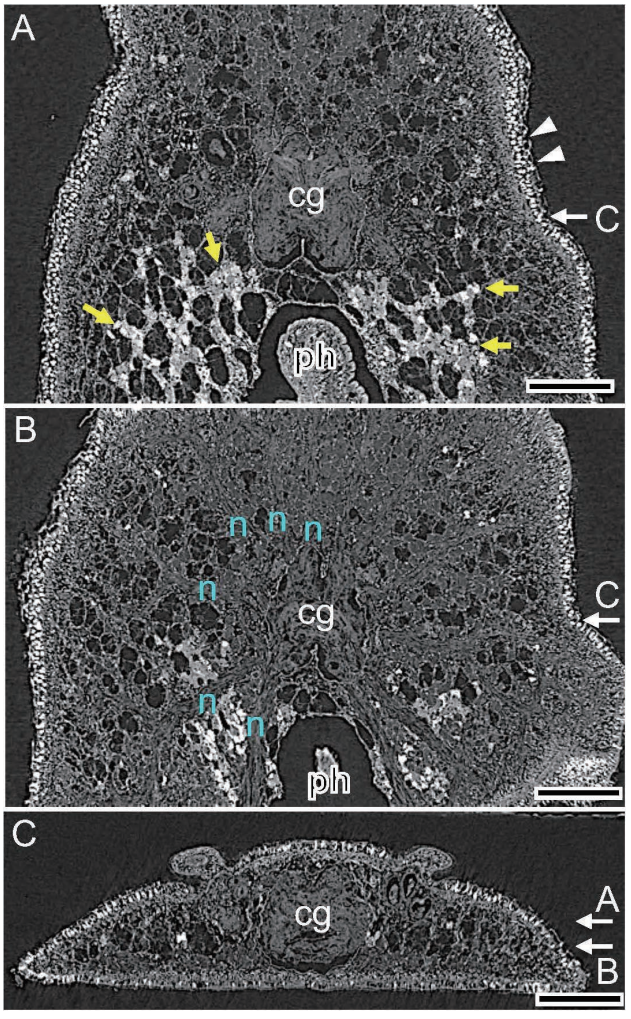

Fig. 2. **(A, B)** Representative horizontal tomographic images of *Stylochoplana pusilla*, including the cephalic ganglion (cg) and pharynx (ph). **(B)** is a more ventral plane image than **(A)**. White arrowheads and yellow arrows in **(A)** indicate higher X-ray absorbents on the surface of the trunk and around the pharynx, respectively. **(B)** Six pairs of nerve cords (n) are connected bilaterally with the more ventral region of the cephalic ganglion. **(C)** Vertical transverse section image of the flatworm cephalic ganglion. White arrows indicate each level of the horizontal sections shown in **(A)** and **(B)**. All images are obtained from the same micro-CT dataset. Scale bars = 100 μm.

Tomographic images showed higher X-ray absorbents distributed on the body surface (Fig. 2A, arrowheads). By comparing images of H-E-stained histological sections (Fig. 1E), we conclude that these cells are likely to be glandular epithelial cells including abundant mucus. In addition, numerous higher X-ray-absorbent cells were scattered radially and peripherally around the pharynx, which contains a large amount of mucus (Fig. 2A, yellow arrows).

Characterization of the mushroom body-like structure adjacent to the cephalic ganglion

In the region antero-lateral/dorsal to the cephalic ganglion, globuli cell masses and lobes of a mushroom body-like structure (Wolff and Strausfield, 2015) were present (Fig. 3). Figure 3A shows a fluorescence image of a horizontal paraffin section of an *S. pusilla* cephalic ganglion labeled with DAPI (green) and anti-synapsin immunocytochemistry (magenta). Dense small-cell nuclear masses labeled with DAPI were located in the mushroom body-like structures (Fig. 3A, yellow arrows).

In horizontal plane micro-CT images, these globuli cell masses could be recognized adjacent to the anterior part of the cephalic ganglion (Fig. 3B, yellow arrows). Observation of the serial sections revealed that, in addition to these cell masses, several putative nerve cords were located in the ventral part of the cephalic ganglion (Fig. 3B1–B4, and see Supplementary Movie S1). In more dorsal regions, nerve bundles extended from the globuli cell masses and projected into the cephalic ganglion (Fig. 3B2–B5, arrowheads). Figure 3C shows a vertical transverse plane image of the cephalic ganglion. As seen in the horizontal plane images (Fig. 3B5), fiber bundles on both sides run dorsally and are joined in the midline, forming a commissure-like structure (Fig. 3C, arrowheads). Because the cephalic ganglion, globuli cell masses of the mushroom body-like structure, and associated nerve fiber bundles could easily be identified in tomographic images, we were able to label them separately and reconstruct 3-D images (Fig. 3D, and see Supplementary Movie S2). The 3-D tomography analysis revealed that the globuli cell masses are located ventro-laterally on the anterior surface of the cephalic ganglion and that the nerve fiber bundles run dorso-medially (Fig. 3D).

Central pathway of optic nerve-like structures

In the micro-CT images, we found, around the cephalic ganglion, several hemispherical structures, which had a higher X-ray absorbance in the core (medulla region) and a cup-like (cortical) structure. These structures were distributed bilaterally dorso-lateral to the cephalic ganglion (Fig. 4A, B, asterisks). From their morphological features and by comparison with gross dorsal view images of *S. pusilla* (Fig. 1), we determined these structures to be the eye-points. We also identified the fiber bundle-like structure that appeared to be derived from these eye-points and which entered the cephalic ganglion (Fig. 4A1–A3, B1, yel-

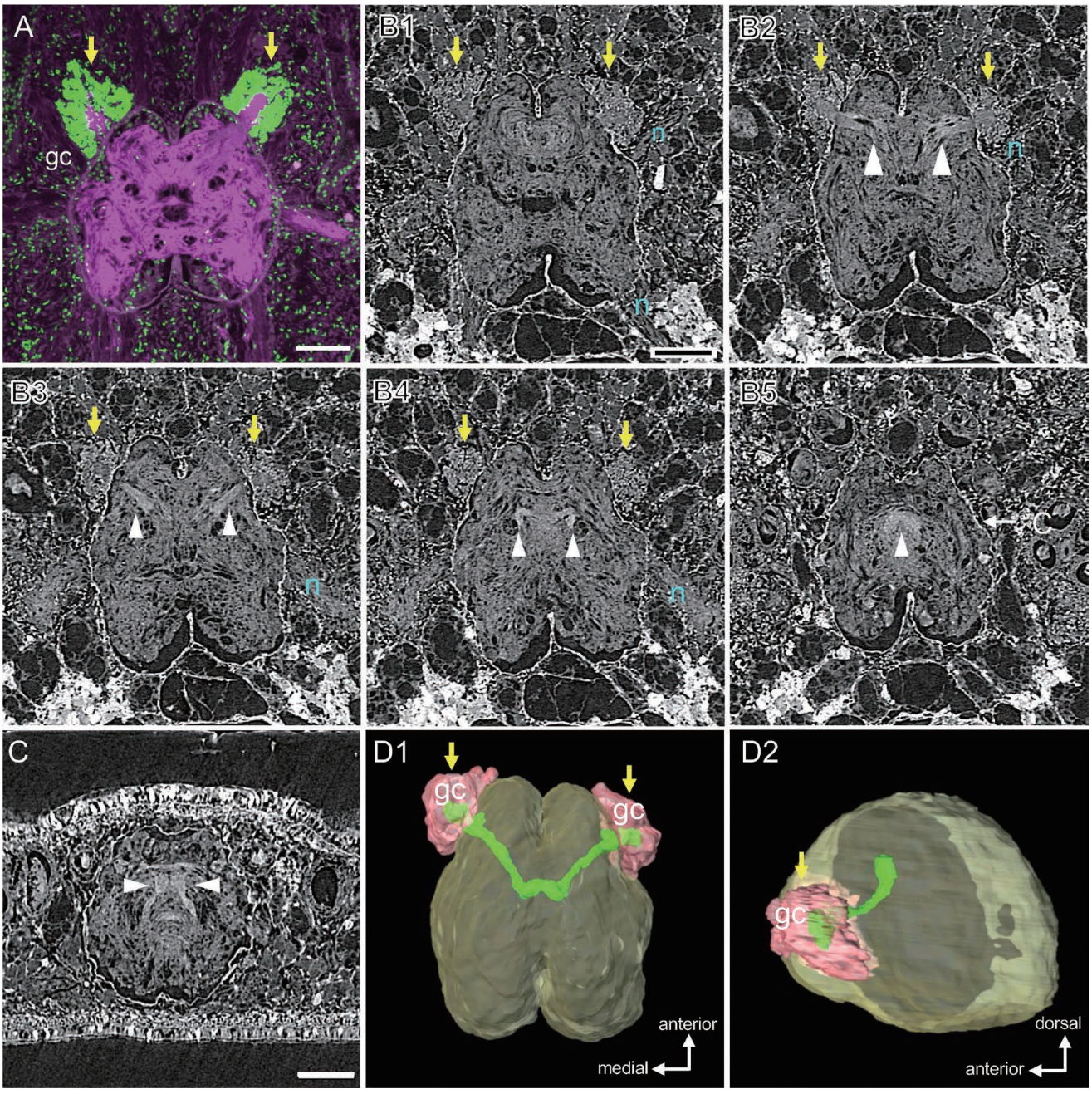

Fig. 3. Micro-CT images of the mushroom body-like structure attached to the cephalic ganglion of *Stylochoplana pusilla*. **(A)** Fluorescence image of horizontal section in the flatworm cephalic ganglion region: globuli cells (gc) are stained by DAPI (green); the cephalic ganglion region by anti-synapsin antibody (magenta). **(B)** Tomographic images of horizontal sections of the cephalic ganglion, including globuli cells (yellow arrows) and nerve bundles (lobes, white arrowheads). These images are obtained from a single micro-CT dataset. **(B1)** is ventral and **(B5)** is dorsal. The white arrow in **(B5)** indicates the section level shown in **(C)**. **(C)** Tomographic image of a vertical transverse section of cephalic ganglion at the antero-posterior level indicated by the white arrow in **(B5)**. White arrowheads indicate a nerve bundle-like structure, as seen in **(B)**. **(D)** Reconstructed 3-D images of the cephalic ganglion (ochre), globuli cells (pink) and nerve bundles (green) of *S. pusilla*. **(D1)** is the dorsal view, and **(D2)** is the lateral view. n: nerve cord. Scale bars = 50 μm.

low arrows). These putative optic-nerve bundles projected antero-medially (Fig. 4A3) and then became associated at the midline (putative optic commissure-like structure) (Fig. 4A4–A6, B2, arrowheads, and see Supplementary Movie S1). The 3-D reconstructed images also showed that the putative optic nerve bundles ran anteriorly and were most likely associated medially with the cephalic ganglion (Fig. 4C, and see Supplementary Movie S2). From the observation of the reconstructed 3-D structure, we found that the putative optic nerves (magenta) were located more dorsally than the nerve cords associated with the mushroom body-like organ (green) (Fig. 4D, and see Supplementary Movie S2).

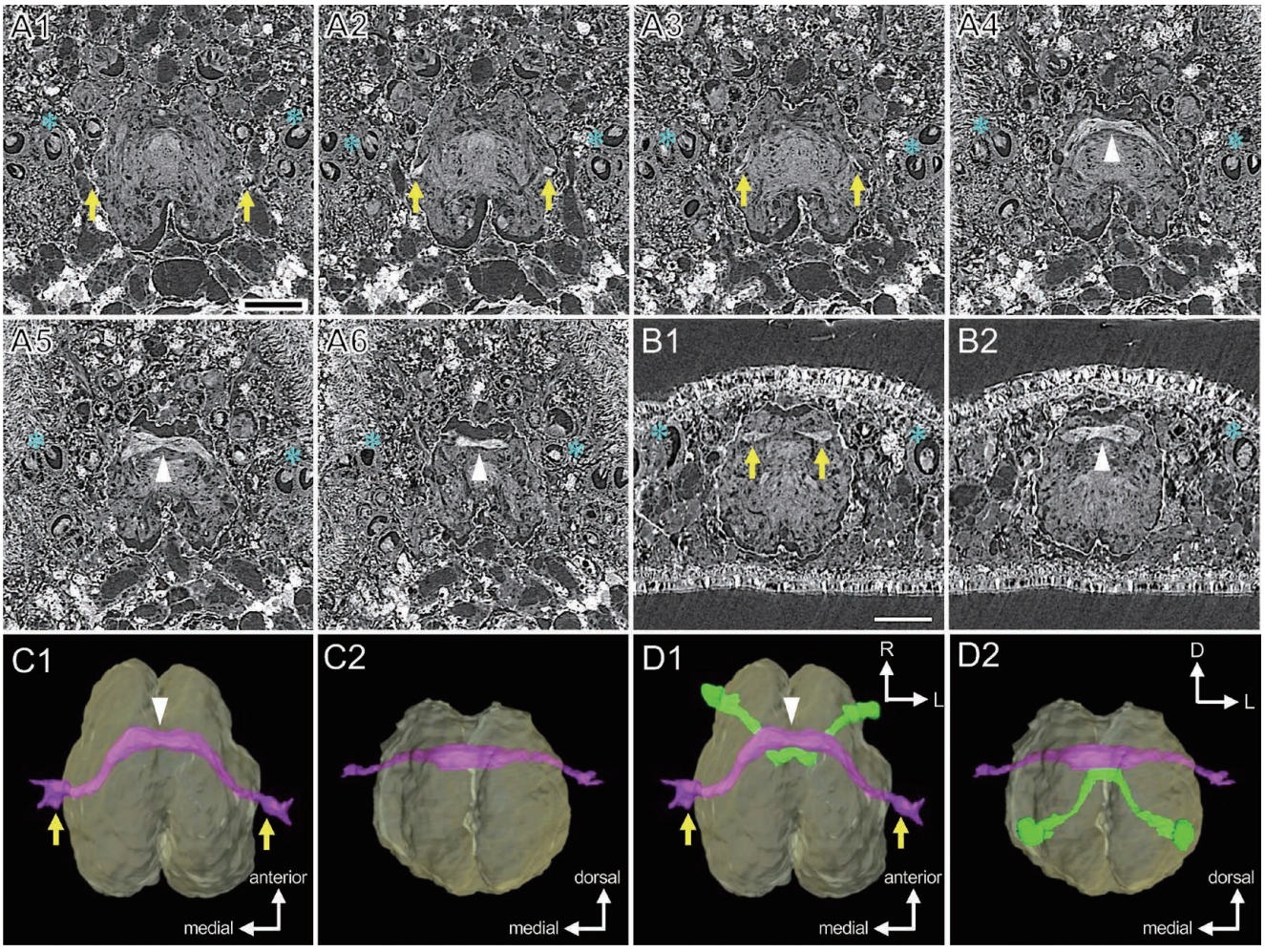

Fig. 4. Central pathway of putative optic nerves in micro-CT images in *Stylochoplana pusilla*. **(A)** Tomographic images of the flatworm cephalic ganglion horizontal sections, including putative optic nerves (yellow arrows). White arrowheads indicate the midline joining of putative optic nerves. Cyan asterisks indicate examples of putative eye-points. These images are obtained from a single micro-CT dataset. **(B)** Tomographic images of the cephalic ganglion vertical transverse sections, including nerve bundles. Yellow arrows in **(B1)** and white arrowhead in **(B2)** indicate separated and joined nerve bundles, respectively. **(C, D)** Reconstructed 3-D images of the cephalic ganglion (ochre), putative optic nerve (magenta), and nerve bundles (lobes) (green) associated with the putative mushroom-body-like structures in **(D)**. **(C)** shows 3-D images of putative optic nerves (magenta). **(D)** also shows those of nerve bundles (lobes, green) associated with the putative mushroom body-like structures. **(C1)** and **(D1)** are the dorsal views, and **(C2)** and **(D2)** are the frontal views. Scale bars = 50 μm.

DISCUSSION

Recently, X-ray micro-CT imaging in synchrotron radiation facilities has been performed to acquire high-resolution CT images of both vertebrates and invertebrates (Mizutani et al., 2007, 2013, 2016). A previous report indicated that the PTA methodology produces high-contrast images of soft tissue in conventional micro-CT (Metscher, 2009). We carried out PTA staining in fish brains in a similar way to this study for micro-CT imaging by SPring-8, and found no observable tissue shrinkage in these brains (Ikenaga et al., 2022). In the present study, we performed micro-CT scanning of a PTA-contrasted marine flatworm, *S. pusilla*, as a simple bilaterian organism with a centralized nervous system (Quiroga et al., 2015). We found that the tomographic images obtained were sufficient to discriminate some characteristic structures of the nervous system. The cephalized central nervous tissue (cephalic ganglion) has been suggested to be a homologous structure to brains in other bilaterians, such as vertebrates (Keenan et al., 1981; Quiroga et al., 2015; Strausfeld et al., 2016; Heger et al., 2021; Martin-Duran and Hejnol, 2021). In addition, the marine flatworm 'brain' appears to be enclosed by a capsule-like structure (Quiroga et al., 2015), which appears to be a homologous structure to the meninges in vertebrates. Six radially extending pairs of nerve cords were identifiable around the cephalic ganglion, as reported previously using dozens of serial paraffin sections (Quiroga et al., 2015). We could also identify mushroom body-like structures, including globuli cell masses and the associated nerve bundles (possibly lobes), which are characteristic of the mushroom bodies of insects and crustaceans (Wolff and Strausfield, 2015). Furthermore, putative optic nerves could be distinguished in 3-D, and appear to form an optic commissure-like structure, as discovered in a freshwater

planarian using arrestin-immunocytochemistry (marker for planarian optic nerve fibers) (Yamamoto and Agata, 2011).

In addition to the nervous system, epithelial cells in the body surface, putative glandular cells, were identified in our virtual CT 2-D images (Fig. 2). Around the pharynx, cells showing higher X-ray absorbance (probably due to the abundance of mucus) were radially distributed (Fig. 2A, yellow arrows). These cells might be glandular cells involved in digestion or smooth muscle cells oriented vertically, and further characterization is necessary. X-ray micro-CT imaging of a number of invertebrate species stained with various chemical agents has been reported (Faulwetter et al., 2013; Steinhoff et al., 2017; Maeno et al., 2019; Sakurai and Ikeda, 2019; Rivera-Quiroz and Miller, 2022). Although these studies provided 3-D images of multiple components, few showed the single cell-resolution image reported in our study. It is, therefore, essential to extend the present micro-CT tomography in synchrotron radiation facilities to other non-model organisms to advance their efficient morphological characterization.

Through the micro-CT imaging, we obtained undistorted serial section images of the flatworm nervous system (Figs. 2–4, and see Supplementary Movies S1, S2). These serial section images, therefore, permit the visualization of precise spatial relationships of neuronal subpopulations and/or nerve tracts potentially as an alternative connectome. For example, the 3-D tracts of nerve bundles associated with the lobes of putative mushroom body-like structures reported in marine polyclad flatworms (Wolff and Strausfield, 2015), but not in freshwater planarians, could be first traced.

Similarly, our reconstruction of the serial 2-D images of the central pathway of the putative optic nerves (Fig. 4A, B) is also informative. We found that bilateral 'optic nerves' run rostro-medially and become anatomically associated in the midline. The serial section images and 3-D movies show that this central joining of 'optic nerves' is located more dorsally than that of lobes of the tracts associated with the putative mushroom body-like structures. The present micro-CT analysis is, therefore, also helpful in validating anatomical stereocrossing.

Micro-CT analysis has been employed in studies involving land planarians, also known as triclad flatworms (Carbayo et al., 2016; Silva et al., 2020). These studies have provided 3-D images of both external and internal structures that corroborate findings from previous taxonomic investigations. However, it is worth noting that the techniques used in these reports present challenges when aiming to analyze cellular details at a high resolution. Consequently, the identification of individual brain neurons at the microscopic level in flatworms remains unattainable. Furthermore, it is important to highlight that the central nervous system of land planarians exhibits similarities with that of freshwater planarians, whereas marine flatworms indicate a greater degree of centralization. In our study, we identified, by using micro-CT in Platyhelminthes, marine polyclad flatworms, both an optic commissure-like structure and putative mushroom body-like structures (Higuchi et al., 2009; Wolff and Strausfield, 2015). In the marine flatworm *Notoplana sanguinea*, high levels of DC0 (insect mushroom body marker) expression have been reported in the mushroom body-like structure (lobe), implying that it is a shared trait of the mushroom body in insects (Wolff and Strausfield, 2015). The existence of functional mushroom bodies in Platyhelminthes is controversial; however, previous reports (Wolff and Strausfield, 2015, 2016) suggest that DC0 is also expressed in the putative mushroom body-like structure in marine flatworms. The mushroom bodies play some roles in learning and memory in insects (Strausfield, 2002). In addition, it is reported that insect mushroom body-related genes (such as DC0, leonardo, and Ca^{2+}/calmodulin-dependent protein kinase II) are also expressed in the putative mushroom body-like structures in several invertebrate species, including Platyhelminthes (Wolff and Strausfield, 2015, 2016). Although further studies on the role(s) of the mushroom body-like structures in *S. pusilla* are needed to understand the origin and diversity of the mushroom body in insects and crustaceans, the analysis of their location, morphology, and specific gene expressions would be informative. Recently, we reported, in marine flatworms, that platytocin, a vasopressin–oxytocin-like neuropeptide of the Platyhelminthes, inhibits gustatory-associated detection-learning (Kobayashi et al., 2022). The putative platytocin receptor, in addition to the ground pattern genes for the insect mushroom body (such as *DC0*, *Leo*, *CaMKII*) (our unpublished observation), is also expressed in the mushroom body-like structure in marine flatworms (Kobayashi et al., 2022). The mushroom body-like structures in marine flatworms may therefore be involved in chemosensory-associated learning.

The optic chiasm is well known in mammals, including humans, and is thought to be an essential structure for stereopsis. However, in the compound/simple eye systems of insects and crustaceans, the left and right optic nerves do not join each other because the structure of the visual system is different from that of mammals. In this study, serial images of horizontal sections of the cephalic ganglion were obtained from a single micro-CT dataset (Fig. 4). These results indicate the midline joining of putative optic nerves. It will therefore be intriguing to determine if any 'optic nerve' fibers cross the midline in *S. pusilla* and where they end. While the optic chiasm-like structure has been reported in freshwater planarians (Yamamoto and Agata, 2011), it is very interesting that both putative optic chiasm and mushroom body-like structures are present in marine polyclad flatworms. Together with the putative mushroom body, these results suggest that the marine flatworm "brain" provides a valuable 'intermediate' between the nervous system in protostomes and the deuterostome brain. The hermaphrodite "brain" might combine elements of the protostome and deuterostome lineages.

ACKNOWLEDGMENTS

We thank Shoko Sekiguchi and Yasuyo Okida (Okayama University) for their technical support. We also thank Professor John F. Morris (University of Oxford) for critically reading the manuscript. This work was supported by Grants-in-Aid for Scientific Research from the Japan Society for the Promotion of Science (JSPS) KAKENHI (to TI: 17K07943, 21K05772; to TS: 20K21429, 21H02520, 22K19312; and to HS: 16H06280, 20K06722, 22H02656, 22K19332), by Grant-in-Aid for Scientific Research on Innovative Areas "Singularity Biology (No. 8007)" of MEXT, Japan (to TS: 21H00428), by the Takeda Science Foundation, Japan (to HS:

Bioscience Research Grants), by the Suzuken Memorial Foundation, Japan (to HS: 19-085), and by the Wesco Scientific Promotion Foundation, Japan (to HS: International Travel Grants; Research Grants).

COMPETING INTERESTS

The authors declare no conflict of interest.

AUTHOR CONTRIBUTIONS

TI and AK performed histological experiments. TI, AT, KU, and HS performed the micro-CT analysis. TM, NS, and TS interpreted the data and provided advice. TI and HS wrote the paper. HS conceived and supervised the whole study. All authors had full access to all of the data in the study and took responsibility for the integrity of the data and the accuracy of the data analysis.

SUPPLEMENTARY MATERIALS

Supplementary materials for this article are available online. (URL: https://doi.org/10.6084/m9.figshare.21862140.v2)

Supplementary Movie S1. The representative movie was obtained from a view of horizontal plane images for the cephalic ganglion. Movie starts from the ventral image.

Supplementary Movie S2. 3-D image of micro-CT of the cephalic ganglion, its associated nerve bundles, and eye-points of *Stylochoplana pusilla*.

REFERENCES

Babaei F, Hong TL, Yeung K, Cheng SH, Lam YW (2016) Contrast-enhanced X-ray micro-computed tomography as a versatile method for anatomical studies of adult zebrafish. Zebrafish 13: 310–316

Bickmeyer U, Meinen I, Meyer S, Kroner S, Brenner M (2020) Fluorescence measurements of the marine flatworm *Macrostomum lignano* during exposure to TNT and its derivatives 2-ADNT and 4-ADNT. Mar Environ Res 161: 105041

Bischof J, Day ME, Miller KA, LaPalme JV, Levin M (2020) Nervous system and tissue polarity dynamically adapt to new morphologies in planaria. Dev Biol 467: 51–65

Camilieri-Asch V, Shaw JA, Yopak KE, Chapuis L, Partridge JC, Collin SP (2020) Volumetric analysis and morphological assessment of the ascending olfactory pathway in an elasmobranch and a teleost using diceCT. Brain Struct Funct 225: 2347–2375

Carbayo F, Lenihan JW (2016) Micro-computed tomography scan and virtual histological slide data for the land planarian *Obama otavioi* (Platyhelminthes). GigaScience 5: 13

Faulwetter S, Vasileiadou A, Kouratoras M, Thanos D, Arvanitidis C (2013) Micro-computed tomography: Introducing new dimensions to taxonomy. Zookeys 263: 1–45

Hayworth KJ, Morgan JL, Schalek R, Berger DR, Hildebrand DG, Lichtman JW (2014) Imaging ATUM ultrathin section libraries with WaferMapper: a multi-scale approach to EM reconstruction of neural circuits. Front Neural Circuits 8: 68

Heger P, Zheng W, Rottmann A, Panfilio KA, Wiehe T (2020) The genetic factors of bilaterian evolution. eLife 9

Henny P, Brown MT, Micklem BR, Magill PJ, Bolam JP (2014) Stereological and ultrastructural quantification of the afferent synaptome of individual neurons. Brain Struct Funct 219: 631–640

Higuchi N, Kohno K, Kadowaki T (2009) Specific retention of the protostome-specific PsGEF may parallel with the evolution of mushroom bodies in insect and lophotrochozoan brains. BMC Biol 7: 21

Ikenaga T, Shimomai R, Hagio H, Kimura S, Matsumoto K, Kato DI, et al. (2022) Morphological analysis of the cerebellum and its efferent system in a basal actinopterygian fish, *Polypterus senegalus*. J Comp Neurol 530: 1231–1246

Keenan CL, Coss R, Koopowitz H (1981) Cytoarchitecture of primitive brains: Golgi studies in flatworms. J Comp Neurol 195: 697–716

Kobayashi A, Hamada M, Yoshida MA, Kobayashi Y, Tsutsui N, Sekiguchi T, et al. (2022) Vasopressin-oxytocin-type signaling is ancient and has a conserved water homeostasis role in euryhaline marine planarians. Sci Adv 8: eabk0331

Le D, Sabry Z, Chandra A, Kristan WB 3rd, Collins ES, Kristan WB Jr (2021) Planarian fragments behave as whole animals. Curr Biol 31: 5111–5117

Maeno A, Kohtsuka H, Takatani K, Nakano H (2019) Microfocus X-ray CT (microCT) Imaging of *Actinia equina* (Cnidaria), *Harmothoe* sp. (Annelida), and *Xenoturbella japonica* (Xenacoelomorpha). J Vis Exp 150: e59161

Martin-Duran JM, Hejnol A (2021) A developmental perspective on the evolution of the nervous system. Dev Biol 475: 181–192

Metscher BD (2009) MicroCT for developmental biology: a versatile tool for high-contrast 3D imaging at histological resolutions. Dev Dyn 238: 632–640

Mizutani R, Suzuki Y (2012) X-ray microtomography in biology. Micron 43: 104–115

Mizutani R, Takeuchi A, Hara T, Uesugi K, Suzuki Y (2007) Computed tomography imaging of the neuronal structure of Drosophila brain. J Synchrotron Radiat 14: 282–287

Mizutani R, Saiga R, Takeuchi A, Uesugi K, Suzuki Y (2013) Three-dimensional network of Drosophila brain hemisphere. J Struct Biol 184: 271–279

Mizutani R, Saiga R, Takekoshi S, Arai M, Takeuchi A, Suzuki Y (2015) Scanning brain networks with micro-CT. Microscopy Today 23: 12–17

Mizutani R, Saiga R, Ohtsuka M, Miura H, Hoshino M, Takeuchi A, Uesugi K (2016) Three-dimensional X-ray visualization of axonal tracts in mouse brain hemisphere. Sci Rep 6: 35061

Pradillon F, Schmidt A, Peplies J, Dubilier N (2007) Species identification of marine invertebrate early stages by whole-larvae in situ hybridisation of 18S ribosomal RNA. Mar Ecol Prog Ser 333: 103–116

Noreña C, Damborenea C, Brusa F (2015) Ecology and general biology. Ch. 10 in “Phylum Platyhelminthes”, 4th ed, Academic Press, London, pp 181–203

Quiroga SY, Carolina Bonilla E, Marcela Bolanos D, Carbayo F, Litvaitis MK, Brown FD (2015) Evolution of flatworm central nervous systems: Insights from polyclads. Genet Mol Biol 38: 233–248

Reuter M, Raikova OI, Gustafsson MK (1998) An endocrine brain? The pattern of FMRF-amide immunoreactivity in Acoela (Plathelminthes). Tissue Cell 30: 57–63

Rivera-Quiroz FA, Miller JA (2022) Micro-CT visualization of the CNS: Performance of different contrast-enhancing techniques for documenting the spider brain. J Comp Neurol 530: 2474–2485

Sakurai Y, Ikeda Y (2019) Development of a contrast-enhanced micro computed tomography protocol for the oval squid (*Sepioteuthis lessoniana*) brain. Microsc Res Tech 82: 1941–1952

Schadt T, Prantl V, Grosbusch AL, Bertemes P, Egger B (2021) Regeneration of the flatworm *Prosthiostomum siphunculus* (Polycladida, Platyhelminthes). Cell Tissue Res 383: 1025–1041

Silva MS, Carbayo F (2020) X-ray microcomputed tomography applied to the taxonomic study of rare material: redescriptions of seven of Schirch’s Brazilian species of land planarians (Geoplanidae, Platyhelminthes). ZooKeys 910: 1–42

Steinhoff POM, Sombke A, Liedtke J, Schneider JM, Harzsch S, Uhl G. The synganglion of the jumping spider *Marpissa muscosa* (Arachnida: Salticidae): Insights from histology,

immunohistochemistry and microCT analysis. Arthropod Struct Dev 46: 156–170

Strausfeld NJ (2002) Organization of the honey bee mushroom body: representation of the calyx within the vertical and gamma lobes. J Comp Neurol 450: 4–33

Strausfeld NJ, Hirth F (2016) Introduction to 'Homology and convergence in nervous system evolution'. Philos Trans R Soc Lond B Biol Sci 371: 20150034

Udagawa S, Miyara K, Takekata H, Takeuchi Y, Takemura A (2019) Investigation on the validity of 3D micro-CT imaging in the fish brain. J Neurosci Methods 328: 108416

Wolff GH, Strausfeld NJ (2015) Genealogical correspondence of mushroom bodies across invertebrate phyla. Curr Biol 25: 38–44

Wolff GH, Strausfeld NJ (2016) Genealogical correspondence of a forebrain centre implies an executive brain in the protostome-deuterostome bilaterian ancestor. Philos Trans R Soc Lond B Biol Sci 371: 20150055

Yamamoto H, Agata K (2011) Optic chiasm formation in planarian I: Cooperative netrin- and robo-mediated signals are required for the early stage of optic chiasm formation. Dev Growth Differ 53: 300–311

(Received August 22, 2023 / Accepted December 29, 2023 / Published online April 8, 2024)